

Supporting information

Enhanced Performance of Dye-Sensitized Solar Cells by Doping Au Nanoparticles into Photoanodes: A Size Effect Study

Qiong Wang,^a Teera Butburee,^a Xia Wu,^a Hongjun Chen,^a Gang Liu^{b,}, and Lianzhou Wang^{a,*}*

^a ARC Centre of Excellence for Functional Nanomaterials, School of Chemical Engineering and Australian Institute for Bioengineering and Nanotechnology, the University of Queensland, St Lucia, Brisbane, QLD, 4072, Australia.

^b Shenyang National Laboratory for Materials Science, Institute of Metal Research, Chinese Academy of Sciences, 72 Wenhua RD, Shenyang 110016, China.

* Corresponding authors. Emails: L Wang, l.wang@uq.edu.au; G. Liu: gangliu@imr.ac.cn

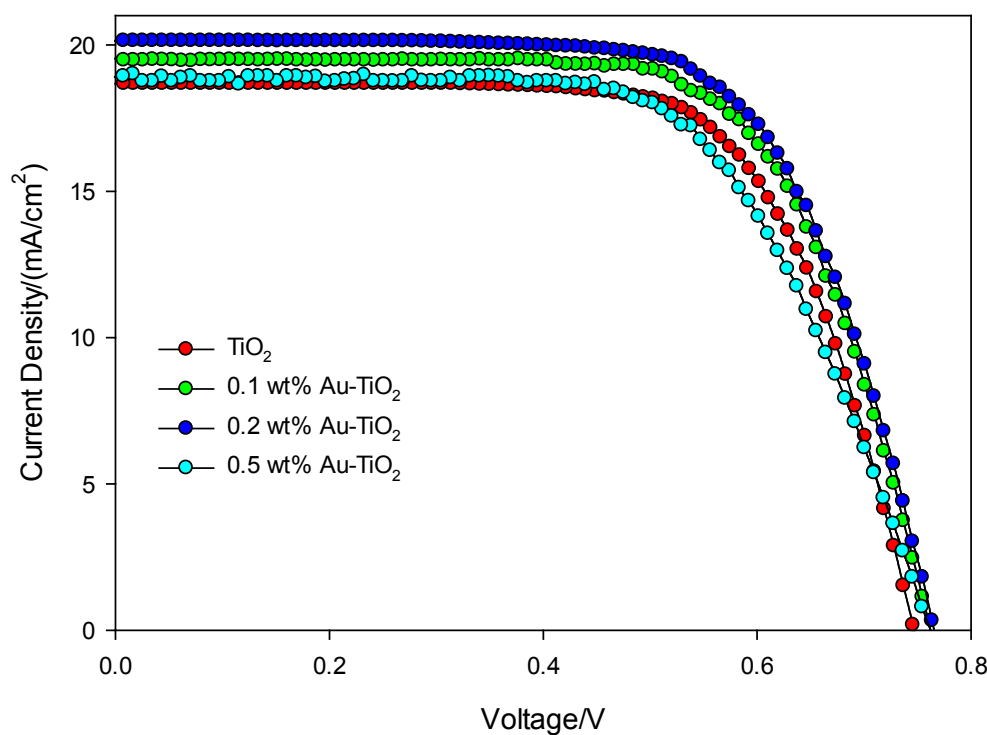


Figure S1. *J-V* curves of DSSCs with different quantities of Au NPs doped inside the photoanodes.

Table S1. Comparison of photovoltaic properties of DSSCs. All measurements were performed under AM 1.5G one sun (light intensity: 100 mW/cm²) and the active area was ca. 0.16 cm² for all cells.

Sample No.	FF	V _{oc} [V]	J _{sc} [mA/cm ²]	η [%]
TiO ₂	0.688	0.747	18.67	9.59
0.1 wt%-Au-TiO ₂	0.684	0.761	19.52	10.17
0.2wt%-Au-TiO ₂	0.685	0.764	20.11	10.52
0.5wt%-Au-TiO ₂	0.644	0.762	18.87	9.26

The $J-V$ curves of DSSCs with different quantities of Au NPs are given in Figure S1, and the photovoltaic performance is summarized in Table S1. From them, we can see that the efficiency of DSSCs is enhanced as the quantity of Au NPs in TiO_2 is increased from 0.1 wt % to 0.2 wt%. However, further increase in the doping amount of Au NPs in TiO_2 results in decrease of the performance of DSSCs. This can be ascribed to the thermal radiation of Au NPs that are excited by incident light, as discussed in reference 24 in the manuscript. Finally, for the size effect study of Au NPs, we fixed the ratio of Au NPs to TiO_2 at 0.2 wt%.

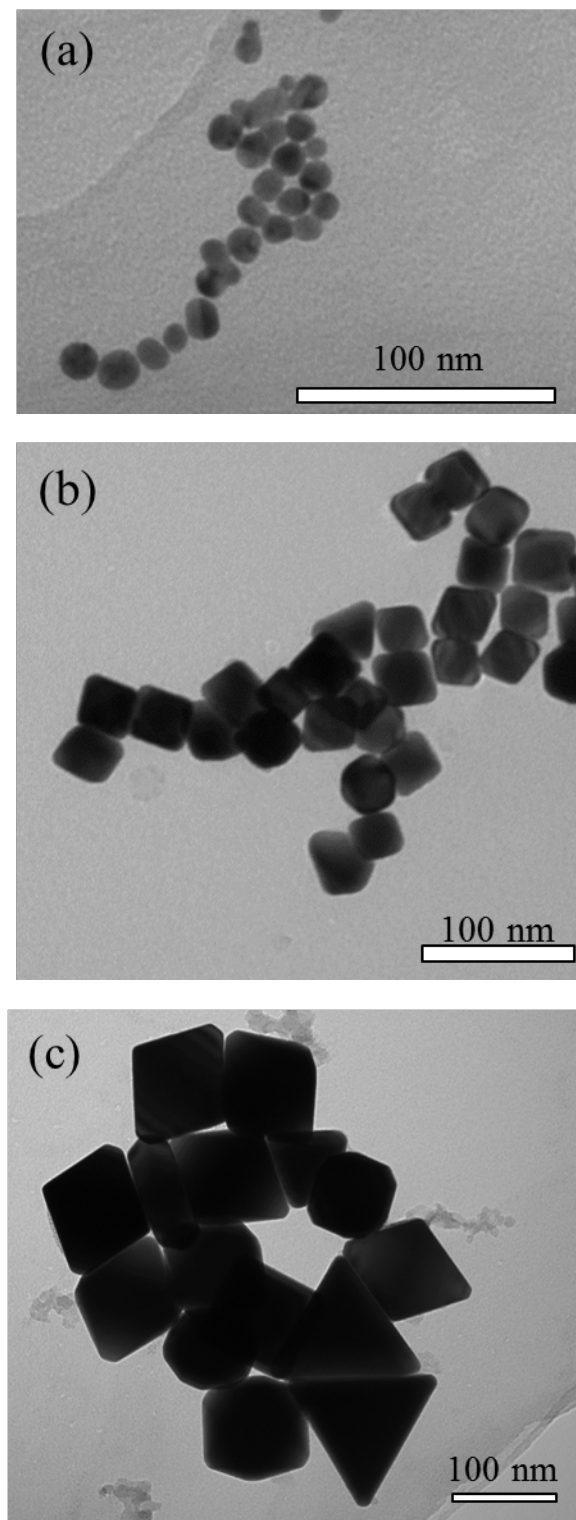


Figure S2. TEM images of spherical Au nanoparticles of around 5 nm (a), and octahedral Au nanoparticles of around 45 nm (b) and 110 nm (c).

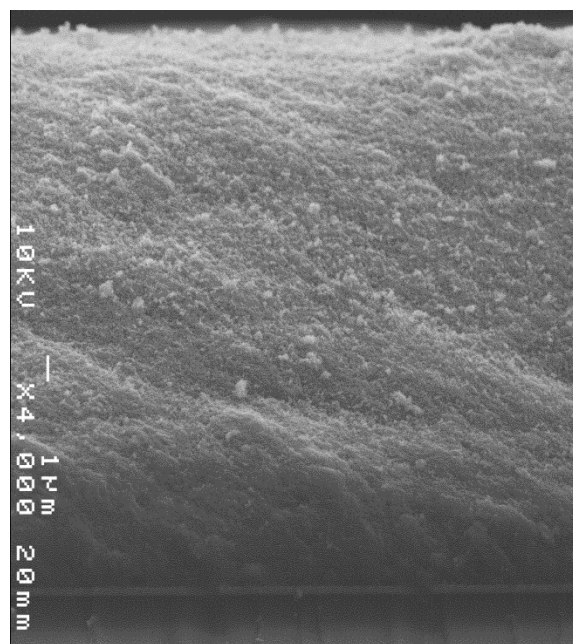


Figure S3a. Cross-sectional SEM image of 5 nm Au-TiO₂ photoanodes.

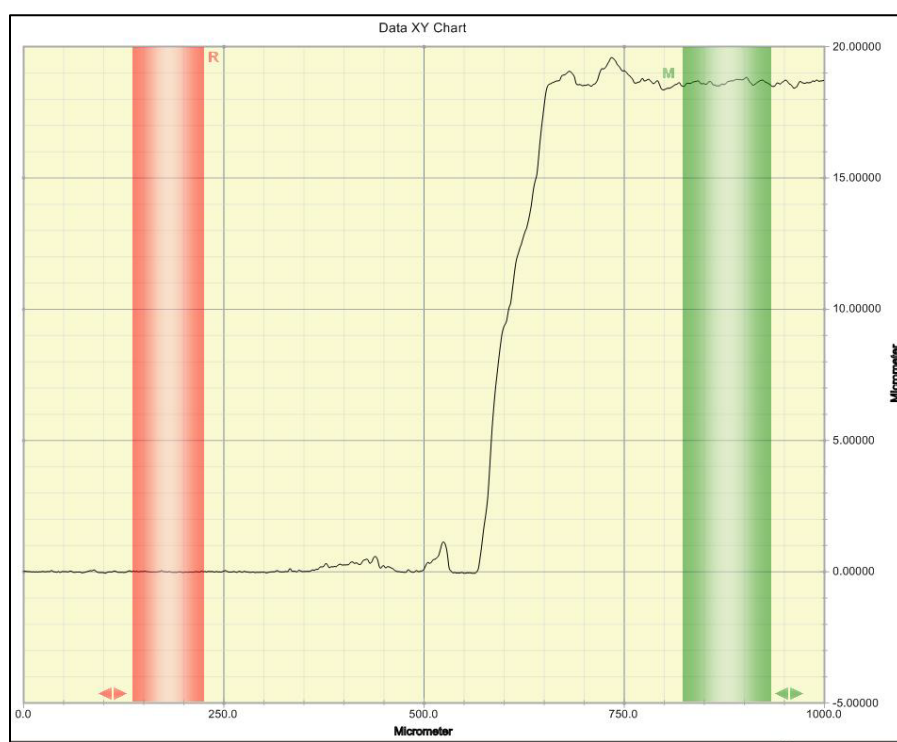


Figure S3b. Film thickness of around 20 μm of 5 nm-Au@TiO₂ photoanodes with 5 nm-Au@TiO₂ as the top layer and TiO₂ as the bottom layer measured by step-profile meter (Veeco Dektak 150 surface profilometer).

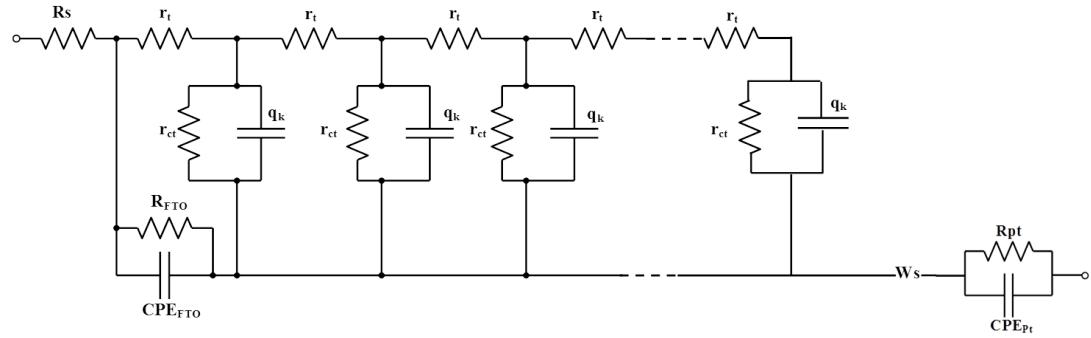


Figure S4a. Complete equivalent circuit employed for the fitting of the EIS spectra of dye-sensitized solar cells.^[1-2]

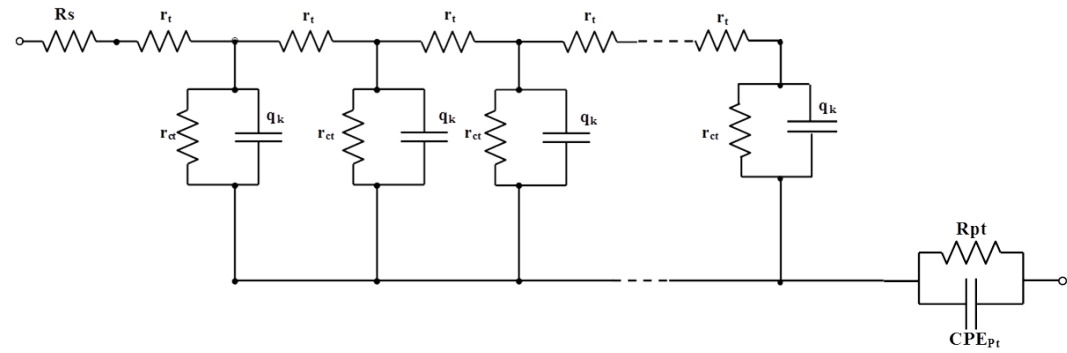


Figure S4b. Simplified equivalent circuit employed for the fitting of the EIS spectra of dye-sensitized solar cells.^[3-4]

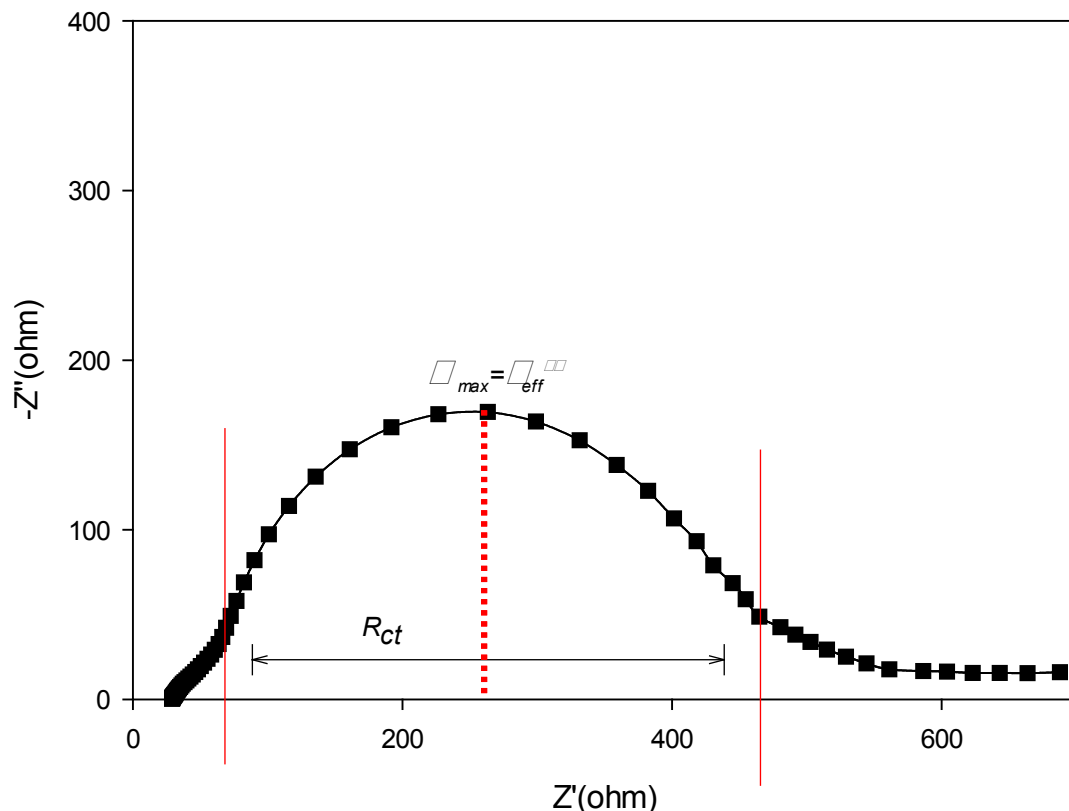


Figure S4c. A typical Nyquist plot of DSSCs obtained from the EIS measurement.

R_s is the series resistance accounting for the transport resistance of the FTO.

R_{FTO} is the charge-transfer resistance for electron recombination from the uncovered layer of the conductive glass (FTO) to the electrolyte.

$R_t (=r_t * L)$ is the electron transport resistance.

$R_{ct} (=r_{ct}/L)$ is the charge-transfer resistance related to recombination of electrons at the TiO_2 /electrolyte interfaces.

R_{pt} is the charge-transfer resistance at the counter electrode/electrolyte interface.

CPE_{FTO} represented the capacitance at the triple contact FTO/ TiO_2 /electrolyte interface.

$CPE_{TiO_2} (=q_k * L)$ is used for the generalization of conventional capacitors for compensation for non-homogeneity in the system, and existed at the TiO_2 nanoparticles and electrolyte interfaces.

CPE_{pt} represented the interfacial capacitance at the counter electrode/electrolyte interfaces.

W_s is the typical finite Warburg impedance of ions diffused in electrolyte.

L is the film thickness of photoanode.

The complex impedance of a cell is the sum of several components, including the contact impedance or resistance (R_s); the impedance at the triple contact FTO/ TiO_2 /electrolyte interface (CPE_{FTO}); the Pt-catalysed counter electrode/electrolyte impedance (CPE_{pt}); the complex impedance which represented the interfaces among TiO_2 /electrolyte (CPE_{TiO_2}); and the diffusion of I_3^- ions impedance (W_s). Normally, the impedance of the I_3^- in the electrolyte is modelled using a finite Warburg element (W_s) which located at the lowest frequency and represented as the third semi-circle in a Nyquist plot. Here in our work, we chose the frequency range from 0.1 Hz to 10^5 Hz, as a result, the typical Warburg impedance was absent. In most cases, the

impedance existed at the triple contact FTO/TiO₂/electrolyte interface is overlapped with other processes and is not easy distinguished. Therefore, the final equivalent circuit exploited for DSSCs is used as given in Figure S3b, and a typical Nyquist plot was given in Figure S3c where the first semi-circle located in high frequency represented the impedance at interface of counter electrode/electrolyte, and the second semi-circle shown in the medium frequency was attributed from the impedance at the interfaces of TiO₂/ electrolyte.

At the interfaces of TiO₂/electrolyte, two important parameters, electron effective lifetime and recombination resistance, can be deduced from the Nyquist plot. As illustrated in Figure S3c, electron effective lifetime, τ_{eff} , and recombination resistance, R_{ct} , are defined as the reciprocal of the peak frequency (ω_{max}) and the diameter of the central arc, respectively.^[5] In a Nyquist plot, Z' and Z'' stands for the real and imaginary part of the impedance. By fitting the Nyquist plot using SAI ZView® software of Scribner Associates Inc, these parameters can be obtained correspondingly.

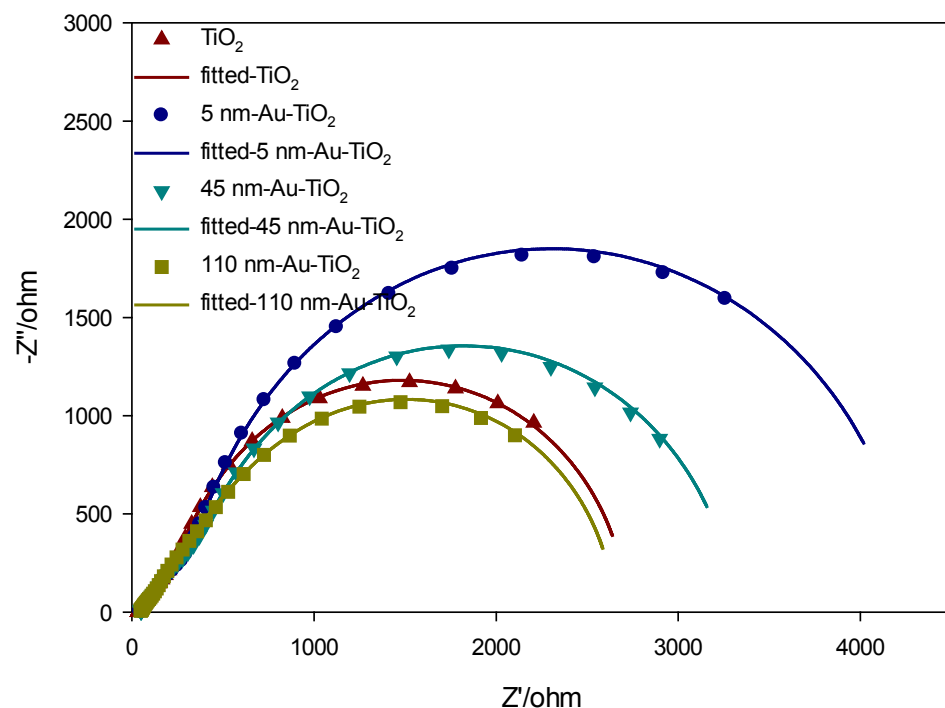


Figure S5. Measured (symbol) and fitted (solid line) Nyquist plots of Au-TiO₂-DSSCs and TiO₂-DSSCs at medium bias voltage of 0.6 V.

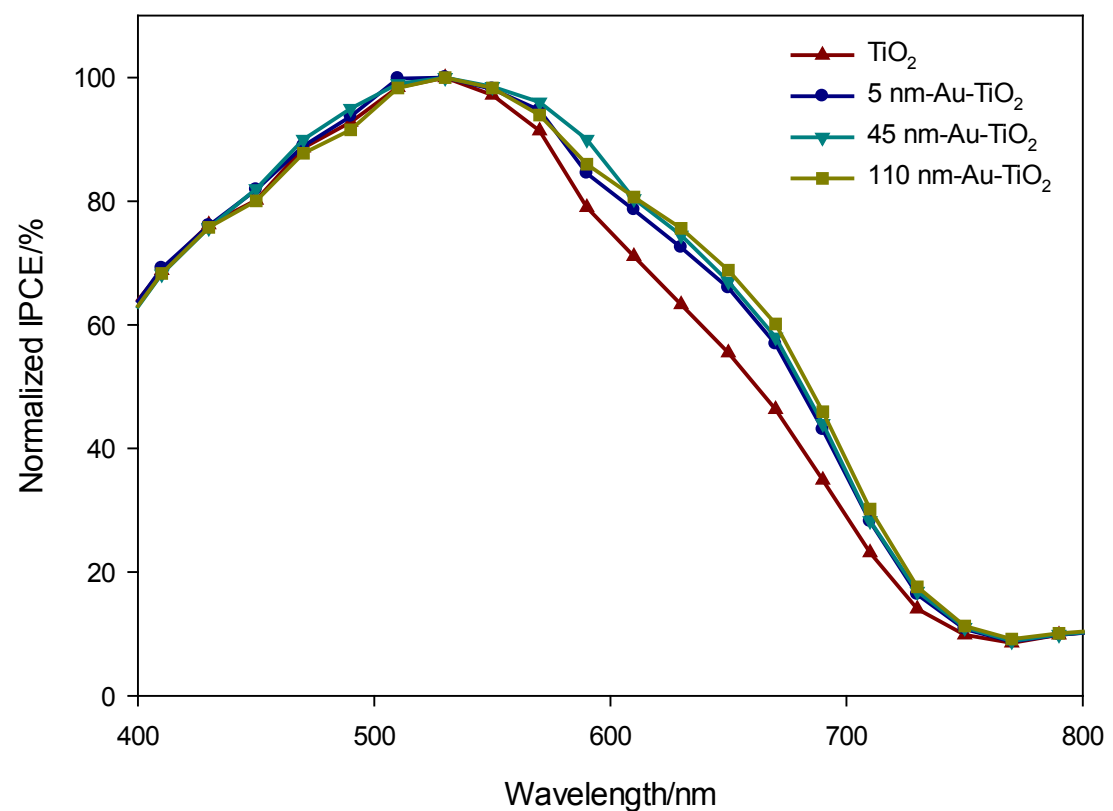


Figure S6. Normalized IPCE spectra of Au- TiO_2 -DSSCs and TiO_2 -DSSCs.

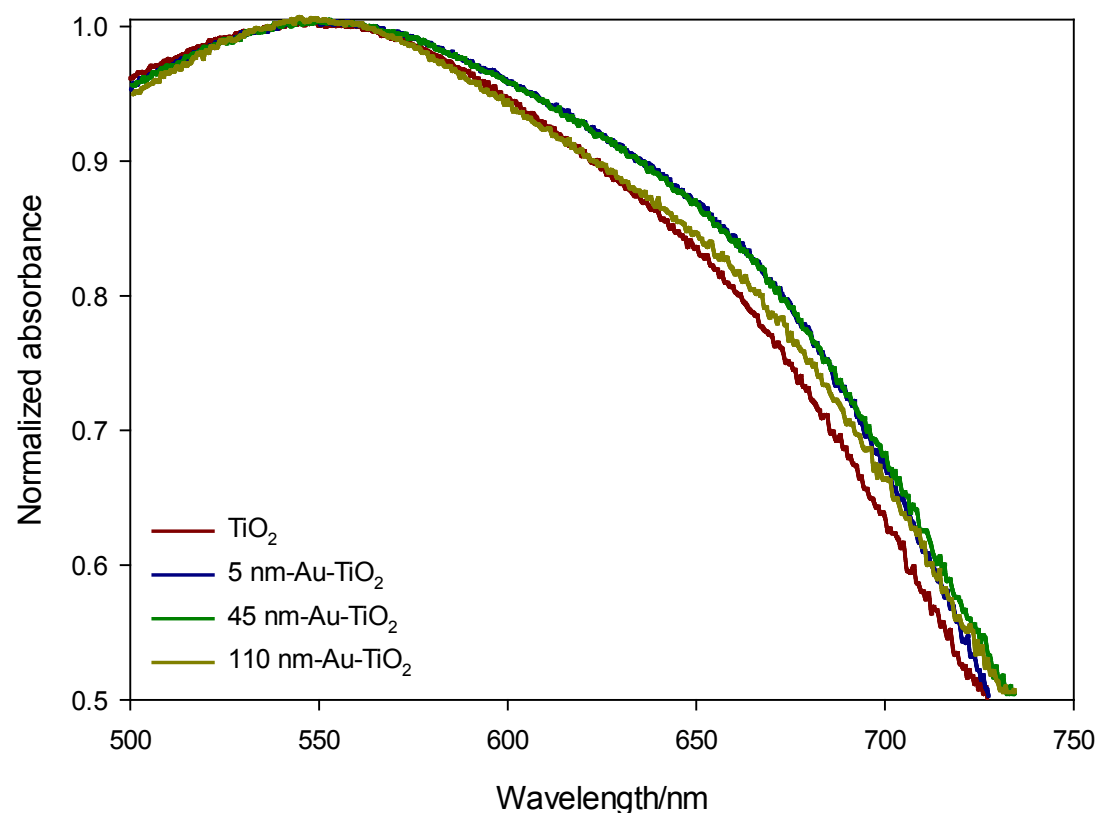


Figure S7. Normalized absorbance spectra calculated as (1-transmittance-reflectance) of dye-loaded photoanodes.

References:

1. A. Zaban, M. Greenshtein and J. Bisquert, *Chemphyschem*, 2003, **4**, 859-864.
2. J. Bisquert, A. Zaban, M. Greenshtein and I. Mora-Sero, *Journal of the American Chemical Society*, 2004, **126**, 13550-13559.
3. Q. Wang, S. Ito, M. Gratzel, F. Fabregat-Santiago, I. Mora-Sero, J. Bisquert, T. Bessho and H. Imai, *J Phys Chem B*, 2006, **110**, 25210-25221.
4. V. González-Pedro, X. Xu, I. Mora-Seró and J. Bisquert, *Acs Nano*, 2010, **4**, 5783-5790.
5. M. Adachi, M. Sakamoto, J. T. Jiu, Y. Ogata and S. Isoda, *J Phys Chem B*, 2006, **110**, 13872-13880.